Multiplicity distribution and source deformation in full-overlap U+U collisions

Anthony Kuhlman and Ulrich Heinz*
Department of Physics, The Ohio State University, Columbus, OH 43210, USA
(Dated: February 9, 2008)

We present a full Monte Carlo simulation of the multiplicity and eccentricity distributions in U+U collisions at $\sqrt{s} = 200\,A$ GeV. While unavoidable trigger inefficiencies in selecting full-overlap U+U collisions cause significant modifications of the multiplicity distribution shown in [1], a selection of source eccentricities by cutting the multiplicity distribution is still possible.

PACS numbers: 25.75.-q, 25.75.Nq, 12.38.Mh, 12.38.Qk

In [1] we advocated the use of full-overlap collisions between deformed uranium nuclei to probe open questions at the Relativistic Heavy Ion Collider (RHIC). Specifically, such collisions can be used to test the hydrodynamic behavior of elliptic flow to much higher energy densities than currently possible with non-central Au+Au collisions, and the large and strongly deformed reaction zones produced in such collisions will allow for a detailed examination of the path length dependence of the energy lost by a fast parton as it travels through the plasma created in the collision.

The calculations presented in [1] were based on the assumption that full-overlap U+U collisions can be efficiently triggered on by using the zero degree calorimeters (ZDCs) of the RHIC experiments to discriminate against collisions with spectator nucleons flying down the beam pipe. By cutting the multiplicity distribution for the thus selected full-overlap collisions one can further select subevent classes with different spatial deformations of the created fireballs. In this short note we explore these assumptions in more quantitative detail, using a Monte Carlo simulation of the distributions of spectator nucleons and charged particle multiplicity for U+U collisions for arbitrary impact parameter and relative orientation between the two deformed uranium nuclei.

Our calculations are based on a Glauber model parametrization of the initial entropy production in these collisions, with standard Woods-Saxon form for the density distributions of the colliding nuclei (see [2] for details). [Possible modifications arising from Color Glass Condensate (CGC) [3] initial conditions [4] will be shortly discussed at the end [9].] The initial entropy density in the transverse plane at $z = 0$ (with z denoting the beam direction) is determined by a combination of terms proportional to the wounded nucleon ($n_{\rm wn}$) and binary collision ($n_{\rm bc}$) densities:

$$s(\boldsymbol{r}_\perp;\Phi) = \kappa_s\,\left[\alpha\, n_{\rm wn}(\boldsymbol{r}_\perp;\Phi) + (1-\alpha)\, n_{\rm bc}(\boldsymbol{r}_\perp;\Phi)\right]. \quad (1)$$

Here Φ is the angle between the beam direction and symmetry axis of one of the two U nuclei; in full-overlap collisions the symmetry axis of the other U nucleus lies in the same plane and forms an angle of Φ or $\pi-\Phi$ with the beam axis. The normalization constant κ_s in (1) is adjusted to reproduce the charged particle multiplicity density $dN_{\rm ch}/dy$ measured at midrapidity in central $200\,A$ GeV Au+Au collisions at RHIC [5], assuming proportionality of $dN_{\rm ch}/dy$ with the total entropy produced in the transverse plane. The wounded nucleon scaling fraction is tuned to $\alpha = 0.75$ [6] to reproduce the centrality dependence of $dN_{\rm ch}/dy$ (see Figure 1). After fitting κ_s and α to the Au+Au data, we use the same parameters to predict the multiplicities for U+U collisions at the same $\sqrt{s}$. The results for full-overlap U+U collisions are shown in Figure 1 by the dashed line; low (high) multiplicities correspond to side-on-side (tip-on-tip) collisions as indicated, due to their smaller (larger) binary collision contribution.

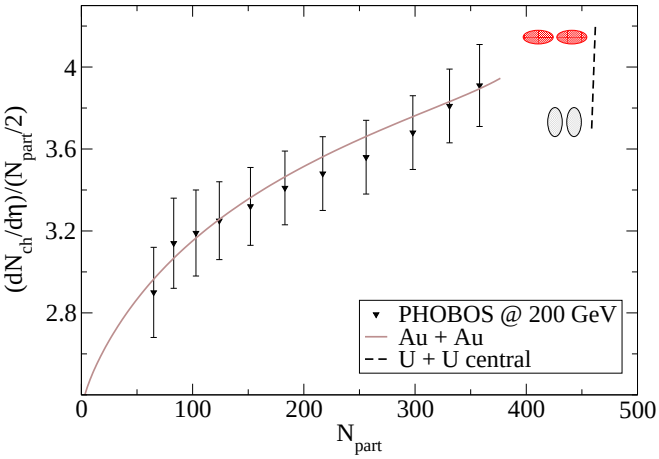

FIG. 1: Multiplicity per participant pair versus the number of participants $N_{\rm part} = \int d^2r_\perp\, n_{\rm wn}(\boldsymbol{r}_\perp)$ for $200\,A$ GeV Au+Au and U+U collisions. Solid line: Glauber model fit to the Au+Au data from PHOBOS [5]. Dashed line: prediction for full-overlap U+U collisions.

To determine the multiplicity distribution, we introduce Gaussian event-by-event fluctuations of the multiplicity $n \equiv dN_{\rm ch}/dy$ via [7]

$$\frac{dP}{dn\; d\Phi} = A\;\exp\left\{-\frac{(n-\bar{n}(\Phi))^2}{2a\bar{n}(\Phi)}\right\}, \quad (2)$$

where $\bar{n}(\Phi)$ is the average charged particle multiplicity computed from Eq. (1) in a U+U collision with orien-

tation angle Φ, and a width of $a = 0.6$ has been shown to yield good agreement with PHOBOS data [7]. The multiplicity distribution is then obtained by integrating (2) over Φ. The resulting distribution [1] is shown by the gray line in Figure 3 below. Its double hump structure results from the Jacobian $d\bar{n}/d\Phi$, and its asymmetry is a consequence of the fluctuation width being proportional to the mean multiplicity $\bar{n}$. Note that the non-linear dependence of the charged multiplicity on the number of participant (wounded) nucleons, arising from the binary collision component in our parametrization (1), leads to a $\sim$ 15% variation of the charged particle multiplicity among full-overlap U+U collisions as the relative orientation of their symmetry axes is varied over the accessible range.

The calculations of multiplicity and eccentricity distributions presented in [1] rely on the assumption that, by monitoring spectator neutrons in the backward and forward zero degree calorimeters (ZDCs) of the RHIC experiments, full-overlap collisions can be perfectly distinguished from those collisions where the two nuclei are slightly misaligned. This is impossible in practice since even fully aligned collisions in general have a small number of spectator nucleons, arising from the dilute nuclear surface, and this number is larger for side-on-side than for tip-on-tip collisions (see Figure 1). Therefore, slightly misaligned tip-on-tip and fully aligned side-on-side collisions can have the same $N_{\rm part}$ and the same ZDC signal. To assess the contamination from collisions with imperfect overlap on the multiplicity and eccentricity distributions requires a more comprehensive study which includes non-central U+U collisions. This is the point of this short note.

A general U+U collision is parametrized by 5 parameters, the impact parameter b and two Euler angles $\Omega = (\Phi, \beta)$ for each nucleus describing the orientation of its symmetry axis relative to the beam axis and impact parameter direction. Equation (1) for the initial entropy density must therefore be generalized to

$$s(\boldsymbol{r}_\perp; b, \Omega_1, \Omega_2) = \kappa_s \left[\alpha\, n_{\rm wn}(\boldsymbol{r}_\perp; b, \Omega_1, \Omega_2) + (1-\alpha)\, n_{\rm bc}(\boldsymbol{r}_\perp; b, \Omega_1, \Omega_2)\right]. \quad (3)$$

The multiplicity distribution is then calculated from

$$\frac{dP}{dn} = A' \int b\, db\, d^2\Omega_1\, d^2\Omega_2 \exp\left\{-\frac{(n-\bar{n}(b,\Omega_1,\Omega_2))^2}{2a\bar{n}(b,\Omega_1,\Omega_2)}\right\}. \quad (4)$$

Evaluating this 5-dimensional integral by Monte Carlo integration, we obtain the multiplicity distribution shown in Figure 2. Its right-most part contains the full-overlap collisions.

We can now try to select the latter from the overall event population by placing stringent cuts on the number of spectators ($= 2 \times 238 - N_{\rm part}$). The distribution of the number of spectators is shown in Figure 5 below.

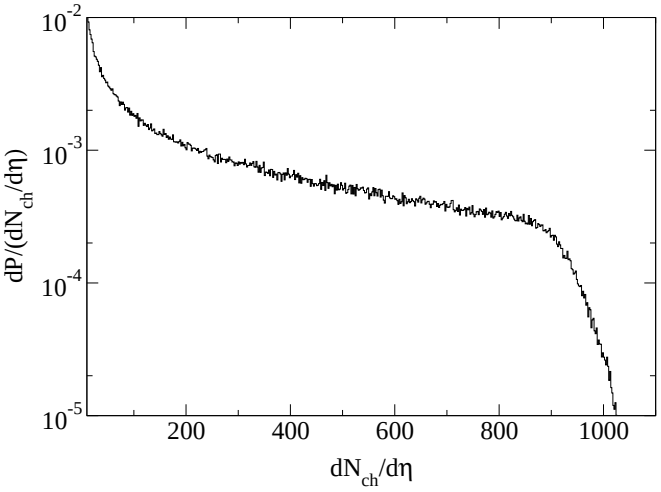

FIG. 2: Multiplicity distribution (normalized to unit total probability) for $\sqrt{s} = 200\,A$ GeV U+U collisions. The distribution was generated from an impact parameter weighted sum of approximately 200,000 events with all possible orientations and impact parameters between the two nuclei.

In Figure 3 we show the multiplicity distributions associated with the 5% and 0.5%, respectively, of events with the lowest spectator counts [8]. It is immediately obvious that contamination from slightly misaligned collisions is sufficient to completely destroy the double-hump structure of the ideal full-overlap case, replacing it with a single peak. By selecting low-spectator events, we bias

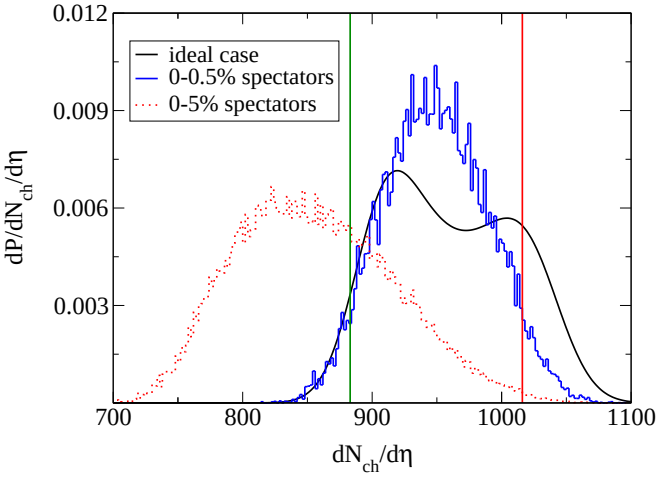

FIG. 3: Multiplicity distribution for the ideal case of only full-overlap collisions (gray line), and for the 0.5% and 5% U+U collision events with the lowest spectator counts (solid blue and dotted red histograms, respectively). All distributions are normalized to unit total probability. The vertical lines indicate 5% and 95% cuts on the blue multiplicity distribution for the 0.5% spectators event class.

the sample towards events with $b \approx 0$, $\Phi_{1,2} \approx 0$, and

the symmetry axes of the two nuclei approximately parallel. This suppresses the contribution from side-on-side configurations under the left peak of the idealized double-hump structure. At the same time, slightly misaligned tip-on-tip collisions fill in the dip between the two humps from the idealized case [9]. The result is a single-peaked multiplicity distribution whose center moves left (towards lower multiplicities) as the cut on the number of spectator nucleons is loosened.

Nevertheless, for sufficiently tight spectator cuts, we still expect the collision events corresponding to the left edge of the multiplicity distributions shown in Figure 3 to have a larger contribution from strongly deformed side-on-side collisions than the events from the right edge (which will be mostly tip-on-tip collisions with small or zero source eccentricity). Following our previous suggestion [1] to select source eccentricities by cutting the multiplicity distribution of "zero spectator" collisions, we perform such cuts on the more realistic distributions shown in Figure 3. Figure 4 shows that it still possible in this way to select event classes with a given average source eccentricity: By taking the 0.5% of events with the lowest spectator count from Figure 3 (solid histogram) and cutting once more on the 5% of events with the *lowest multiplicity*, we obtain the eccentricity distribution shown by the black histogram in the bottom panel of Figure 4. This event class has an average source deformation ϵ_x of about 18%, corresponding to Au+Au collisions with impact parameters around 5.5 fm. On the other hand, taking the same 0.5% spectator cut and selecting the 5% events with the *largest multiplicities* we obtain for the eccentricity distribution the gray histogram in the bottom Figure 4; this distribution peaks at $\epsilon_x = 0$ and has a very small average spatial deformation.

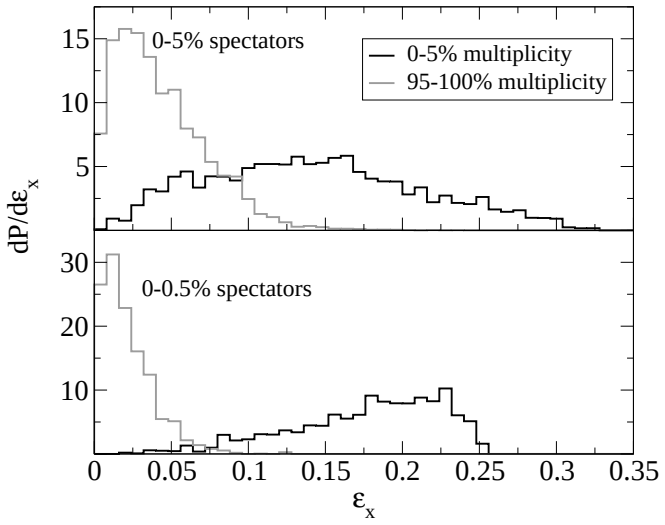

FIG. 4: Normalized eccentricity distributions, after making cuts on the multiplicity distributions for the two event classes shown in Figure 3 (top panel: 5% spectator cut; bottom panel: 0.5% spectator cut). Looser spectator cuts lead to broader eccentricity distributions and less well-defined average eccentricities.

If one loosens the spectator cut to 5% instead of 0.5% (dotted histogram in Figure 3) and performs the same multiplicity selections (5% lowest or largest multiplicities, respectively), one obtains the eccentricity distributions shown in the top panel of Figure 4. Clearly, these distributions are much broader than with the tighter spectator cut, and the average eccentricities shift down from 17.7% to 14.2% for the low-multiplicity selection and up from 2.2% to 4.3% for the high-multiplicity selection. Note that, since the looser spectator cut allows for an increased contribution from non-zero impact parameters, the eccentricity of the nuclear overlap region can actually exceed the $\approx 25\%$ ground state deformation of the single-uranium density distribution projected on the transverse plane. This gives rise to the right tail of the black histogram in the top panel of Figure 4. A typical event from this tail is shown in Figure 5. One sees that the 5% spectator cut allows for sizeable nonzero impact parameters and numbers of spectator nucleons, and that very tight ZDC cuts are required to ensure almost full overlap of the two uranium nuclei.

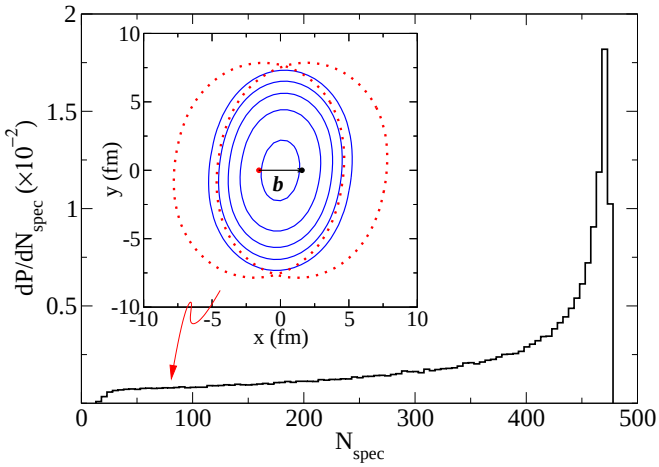

FIG. 5: Distribution of spectator nucleons for 200 A GeV U+U collisions [8]. The inset shows initial entropy density contours ($s = 20$, 40, 60, 80, 100 fm^{-3} from the outside in) for a high-eccentricity event ($\epsilon_x = 0.325$) which is included in a "5% spectator cut" event sample, as indicated by the arrow. The impact parameter of this collision is $b = 3.14$ fm, and it produces $N_{\rm spec} = 87$ spectator nucleons.

The detailed shapes of the eccentricity distributions shown in Figure 4 are expected to depend somewhat on our parametrization (1,3) of the initial transverse density distribution of the produced matter. It was shown in Ref. [4] that initial conditions motivated by the Color Glass Condensate picture of low-x gluon saturation in large nuclei at high energies [3] produce transverse density distributions which fall off more steeply near the edge

than the more Gaussian-like distributions [11] resulting from our Eqs. (1,3). This might result in somewhat larger eccentricities and narrower eccentricity distributions (i.e. better defined average eccentricities) than those shown in Figure 4. However, significantly higher statistics would likely be needed to clearly see such differences.

These results show that the suggestions made in [1] for using U+U collisions to explore in more detail the ideal fluid dynamic nature of elliptic flow and the path length dependence of radiative parton energy loss are reasonably robust against trigger inefficiencies, and that a meaningful U+U collision program at RHIC is, in fact, feasible [12]. Simultaneous strict cuts on small numbers of spectator nucleons and on charged particle multiplicity are necessary to select collisions which produce sources with well-defined and large spatial deformation; the histograms shown in the bottom panel of Figure 4 correspond to only 0.025% of all U+U collisions taking place in the accelerator. The top panel in Figure 4 shows that it is possible to loosen these tight cuts somewhat, at the expense of reducing the average spatial source deformation and introducing larger event-by-event fluctuations as well as an increased sensitivity to details of the Glauber model used for relating the relative nuclear orientation to the observed spectator nucleon and charged hadron multiplicities. We leave a further discussion of such model uncertainties (see also [9]) for later when U+U collisions become (hopefully) available.

We thank M. Gyulassy for stimulating discussions and G. Fai for an enlightening question which led to the discovery of an error in Eq. (4) in the originally submitted manuscript. This work was supported by the U.S. Department of Energy under contract DE-FG02-01ER41190.

* Correspond to heinz@mps.ohio-state.edu

[1] U. Heinz and A. Kuhlman, Phys. Rev. Lett. **94**, 132301 (2005).
[2] P. F. Kolb, J. Sollfrank, and U. Heinz, Phys. Rev. C **62**, 054909 (2000).
[3] E. Iancu and R. Venugopalan, in *Quark-Gluon Plasma 3*, edited by R. C. Hwa and X.-N. Wang (World Scientific, Singapore, 2004), p. 249.
[4] T. Hirano and Y. Nara, Nucl. Phys. A **743**, 305 (2004).
[5] B. B. Back *et al.* [PHOBOS Collaboration], Phys. Rev. Lett. **89**, 222301 (2002).
[6] P. F. Kolb and U. Heinz, in *Quark-Gluon Plasma 3*, edited by R. C. Hwa and X.-N. Wang (World Scientific, Singapore, 2004), p. 634.
[7] D. Kharzeev and M. Nardi, Phys. Lett. B **507**, 121 (2001).
[8] Our calculations neglect event-by-event fluctuations of the number of spectators in collisions of given impact parameter b and orientations Ω_1, Ω_2. We leave this for a more detailed Monte Carlo simulation when U+U collisions become available.
[9] Note that the qualitative difference between the shapes of the double-hump "ideal case" and single-peak multiplicity distribution for the realistic situation shown in Figure 3 is due to the contamination from slightly off-angle, off-center U+U collisions near the low end of the distribution of *spectator nucleons*, which is calculated from the initial distributions of *nucleons* in the two colliding nuclei. It is thus independent of how we parametrize the distribution of *produced* particles in Eqs. (1) and (3), which need not necessarily reflect the *nucleon* density, i.e. the baryon number distribution of the colliding nuclei, but could instead depend on their low-momentum gluon density distribution [4]. Replacing Eqs. (1,3) by a CGC-motivated distribution (as given, for example, in Refs. [4, 7, 10]) would require an adjustment of the normalization contant κ_s in Eqs. (1,3) in order to maintain the agreement between model and Au+Au collision data in Figure 1, and thus might lead to slightly different predictions for the total charged multiplicity produced in full-overlap U+U collisions (resulting in a horizontal shift of the curves in Figure 3). It would not affect, however, the different shapes of the two multiplicity distributions shown in Figure 3.
[10] D. Kharzeev, E. Levin, and M. Nardi, Phys. Rev. C **71**, 054903 (2005).
[11] P. F. Kolb, U. Heinz, P. Huovinen, K. J. Eskola, and K. Tuominen, Nucl. Phys. A **696**, 197 (2001).
[12] This statement remains true even in view of recently pointed out intricacies [13, 14] of interpreting elliptic flow data for $v_2(p_\perp)$ of different hadronic species which result from the late hadronic redistribution of the total momentum anisotropy generated during the early hydrodynamic evolution. While we expect the additional gain in initial energy and entropy density in full-overlap U+U collisions to significantly improve the chances for ideal fluid dynamical evolution and early saturation of the *total* momentum anisotropy $\epsilon_p = \frac{\langle\langle T^{xx} - T^{yy} \rangle\rangle}{\langle\langle T^{xx} + T^{yy} \rangle\rangle}$ [2], the redistribution of this momentum anisotropy over the different hadron species and over transverse momentum reflects an intricate interplay between thermal and (radial) collective motion which is sensitive to the equation of state and chemical composition (as well as to non-ideal fluid effects caused e.g. by a large hadronic viscosity) during the late hadronic stage of the collision [13, 14]. These issues are independent of the initial energy and entropy density and beyond the scope of the present note.
[13] N. Borghini and J. Y. Ollitrault, nucl-th/0506045.
[14] T. Hirano and M. Gyulassy, nucl-th/0506049.